

Performance of Solar Collector Coupled with Three Fluid Heat Exchanger and Heat Storage System for Simultaneous Water and Space Heating



Rama Chandra Panda, Sudhansu S. Sahoo, Ashok K. Barik, Debjyoti Sahu, Taraprasad Mohapatra, and Auroshis Rout

Nomenclature

FPSC	Flat plate solar collector
STSS	Sensible thermal storage system
NTU	Normal transfer unit
$C_{p \min}, C_{p \max}$	Heat capacity rates
η_{optical}	Optical efficiency
F_R	Heat removal factor
U_L	Overall heat transfer coefficient
T_a	Ambient temperature
G	Mass flux
d	Equivalent spherical diameter
μ_f	Dynamics viscosity
A_c	Collector area

R. C. Panda
Biju Patnaik University of Technology, Rourkela, Odisha, India

S. S. Sahoo (✉) · A. K. Barik
Department of Mechanical Engineering, Odisha University of Technology and Research,
Bhubaneswar, Odisha, India
e-mail: sudhansu@cet.edu.in; sahoo.sudhansu@gmail.com

D. Sahu
School of Mechanical Engineering, KIIT Deemed to be University, Bhubaneswar, India

T. Mohapatra
Department of Mechanical Engineering, CV Raman Global University, Bhubaneswar, India

A. Rout
Department of Mechanical Engineering, Odisha University of Technology and Research,
Bhubaneswar, Odisha, India

A_p	Aperture area
ω	Hour angle
I_T	Total radiation on horizontal surface
Q_u	Useful heat absorbed

1 Introduction

It is well-known fact that the solar power is free and used in various conventional and non-conventional processes for years [1]. Being a solar-rich country, India is considered one among the technically developed nations for solar PV and solar thermal-related applications for domestic as well as industrial applications. Usually, on solar thermal category, flat plate solar collector (FPSC) is used as energy harvesting device for water heating purposes during day time [2]. This device is being used in rooftops of houses or apartments. Apart from water heating, FPSC is used for space heating, drying, industrial process heating. Mostly, applications requiring less than 100 °C are best to make use of FPSC during daytime. This system is a combination of various sub-systems namely collectors, storage tanks, fluid distribution systems, fluid control and transport systems.

Many research work on heat transfer analysis of flat plate solar collectors and performance have been carried out by scientists and researchers [3]. Optimization of solar power harvesting vis-a-vis heat storage has been explored and reported widely [4]. Like many other researchers, Karim and Hawalder (2004) experientially investigated flat plate solar collectors along with soft computing approach [5]. It is obvious that effective solar energy is available during sunshine hours, however, with use of effective storage system, the solar energy can be used during night time as well [6, 7].

From the few related work on this field reported, it has been observed that few researchers were mainly focused on energy analysis on various models of FPSC or solar water heaters. However, still there are many literature gaps identified such system modifications, combination of storage system analysis with FPSC, etc. Keeping in mind of dilute source of energy and unavailability during night time and applications related to simultaneous water heating and space heating at few places, special kind of system needs to be implemented. Work-related to this kind of system is also rarely mentioned in literature. Hence, present study concentrates on heat transfer modelling and analysis of FPSC with three fluid heat exchangers (TFHE) and sensible thermal storage system (STSS) for region which demand hot water and hot air round the clock. Performance analysis of a thermal system like the flat plate solar collector, heat exchanger and sensible heat storage system is executed and analyzed here using the standard theoretical model. The solar and weather data are used the simulation purposes [8]. The next section describes on mathematical modelling of three sub-systems namely, FPSC, TFHE and STSS in detail.

2 Mathematical Modelling

2.1 Flat Plate Solar Collector (FPSC)

Thermal modelling of solar collectors is presented in this sub-section. FPSC has been considered here for thermodynamic modelling and its performance analysis. A typical FPSC is considered as shown in Fig. 1. Absorber plate, copper tubes, transparent or glazing cover sheets and an insulated box are main components of it. High thermal conductivity-based sheet metal is used as absorber metal brazed with tubes or ducts below it. The surface of absorber plate is either selective coated or black with the objective to maximize heat absorption and reducing emission.

The insulated box provides structural support to the whole system and minimizes the conductive heat losses in side and back sides of the FPSC. The transparent cover or glass cover sheets usually is made of low ferrite glass to maximize the transmissivity and allow sunlight to pass through to the absorber while simultaneously minimizing convective heat loss.

Usually, water like thermic fluid or nanofluid is circulated inside the tubes that are carrying the absorbed heat. The steady-state useful energy of the collector can be approximated using the conventional expression [9, 10].

$$Q_u = \dot{m} c_{pw} (T_{fo} - T_{fi}) = F_R A_p [S - U_L (T_{fi} - T_a)] \tag{1}$$

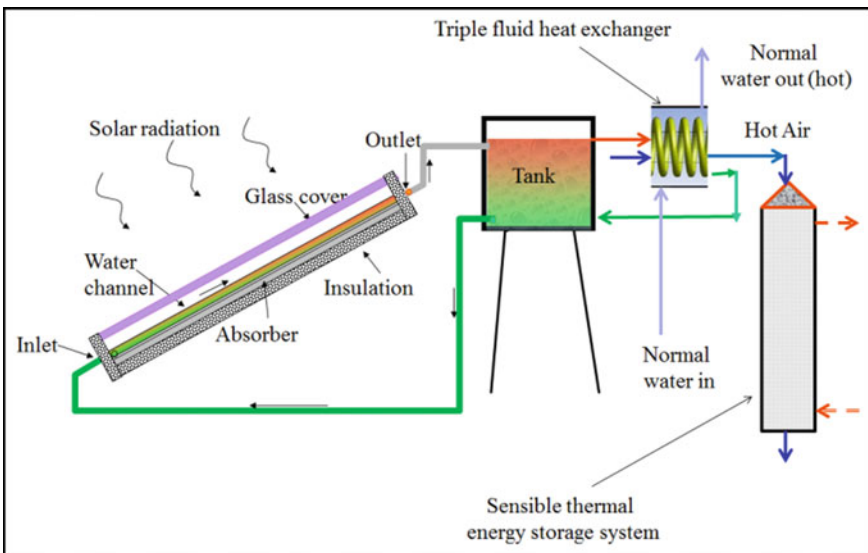


Fig. 1 Pictorial depiction of FPSC with TFHE and STES

Here, by the fluid m , T_{fi} , and T_{fo} are rate of mass flow, inlet and outlet temperature of fluid flowing through the tubes. Heat removal factor is denoted as F_R and overall heat transfer coefficient is mentioned as U_L . T_a can be the ambient temperature. Heat energy absorbed by the absorber plate can be calculated using the expression given in Eq. (2)

$$S = I_T \eta_{opt} \quad (2)$$

The total radiation on horizontal surface is I_T and the optical efficiency of the collector thermal system is $\eta_{optical}$.

Assume tilt factors are almost unity. I_T and H are related by the expression given in Eq. (3).

$$H = \frac{180}{\pi} \sum_{-\omega_s}^{\omega_s} I_T d\omega \quad (3)$$

The hour angle is ω here, can be 15° per hour. The instantaneous thermal efficiency of the collector here by the expression given in Eq. (4).

$$\eta_i = \frac{q_u}{A_C I_T} \quad (4)$$

A_c is the collector area of the FPSC. It is 10% more than aperture area, A_p . The dimensions are mentioned in Table 1.

2.2 Three Fluid Heat Exchanger (TFHE)

In the multi-fluid heat exchanger here, a helical tube is inserted between two straight concentric tubes for hot fluid flow from FPSC tank. Normal water flows through the outer tube/drum and air flows in the centrally located straight tube (Fig. 1). During movement of three fluids in three pipes, heat transfer occurs between them. Heat lost from the hot fluid in helical tube is transferred to water in the outer tube/drum and air in the straight tube. By giving up heat to water carried by outer tube and air, water comes back to FPSC for another cycle. Normal water after gaining heat can be used for domestic applications. Hot air from the TFHE is used for sensible thermal energy storage systems as well as for other applications. Hence the purpose of simultaneous heating of water and air is possible with addition of this TFHE with FPSC.

Energy balance for TFHE can be written as [10]

$$\begin{aligned} \dot{m}c_{pw}(T_{h1} - T_{h2}) \\ = \dot{m}_n c_{pn}(T_{n2} - T_{n1}) + \dot{m}_a c_{pa}(T_{a2} - T_{a1}) \end{aligned} \quad (5)$$

Table 1 Operating and geometrical data of the FPSC with STSS in present work

Items	Value	Items	Value
FPSC		TFHE	
Absorber plate length	2 m	Outer pipe diameter	0.07 m
Absorber plate width	1.13 m	Outer pipe thickness	0.0025 m
Gap between plate and cover	0.025 m	Outer dia. of inner tube	0.0288 m
Plate thermal conductivity	350 W/mK	Thickness of inner tube	0.001 m
Plate thickness	0.00015 m	Outside dia. of helical tube	0.0065 m
Plate absorptivity	0.94	Thickness of inner tube	0.001 m
Plate emissivity	0.14		
Tube outer diameter	0.0137 m	Items	Value
Tube inner diameter	0.0125 m	STSS	
Tube pitch below absorber plate	0.113 m	Cylindrical quartz tube height	1.5 m
glass cover's absorptivity	0.88	Cylindrical quartz tube diameter	0.7 m
Glass cover's Emissivity	0.88	Storage media	Alumina
glass cover thickness	0.04 m	Specific heat	0.88 kJ/kg-K
Adhesive thermal diffusivity	0	Density	3000 kg/m ³
Water flow rate	70 kg/s	Pebble size	3 mm
Water Inlet temperature	60 C	Void fraction	0.4
Ambient temperature	25 C	Initial temperature	20 C
Heat transfer coefficient due to wind effect	16.4 W/m ² K	Mass flow rate to the unit	0.5 kg/s

$$\begin{aligned}
 & \left(\frac{\dot{m}c_{pw}(T_{h1} - T_{h2})}{C_{pmin}(T_{h1} - T_{n1})} \right) \\
 & = \frac{1 - \exp(1 - NTU(1 + C_{pmin}/C_{pmax}))}{1 + C_{pmin}/C_{pmax}} \tag{6}
 \end{aligned}$$

Here T_{h1} , T_{h2} , T_{n1} , T_{n2} , T_{a1} and T_{a2} are temperatures at inlet and outlet of hot water stream, normal water and air streamline, respectively. \dot{m} , \dot{m}_n , \dot{m}_a are mass flow rate of hot fluid, normal fluid and air, respectively. Corresponding specific heats are c_{pw} , c_{pn} and c_{pa} , respectively. C_{pmin} , C_{pmax} are heat capacity rates. NTU is normal transfer unit for considered TFHE. The detailed analysis of TFHE is mentioned in Mohapatra et al. literature[11].

2.3 Sensible Thermal Storage System (STSS)

Thermal modelling of energy storage media is executed and the process, in brief, is presented here. Packed bed type sensible type of storage medium is considered in the present analysis (Fig. 1). It is least complicated compared with latent or chemical storage medium and it is inexpensive. There are drawbacks of course; sensible heat requires large quantities of materials and volumes. A quartz vessel homogeneously but randomly packed (ideally cylindrical) with alumina particles is used as STSS in the present analysis [6]. Alumina beads are mostly spherical. The dimensions are mentioned in Table 1. During charging time, heat supplied to the STSS is stored and during discharging time, the heat is carried by secondary fluid for any applications, mostly during no sun moments or night applications.

The charging and discharging period are in a transient condition. During the charging stage, energy is stored in the thermal energy storage system until the heat storage capacity of the STSS is fully used. Similarly in discharging period, energy recovery takes place. Alumina pebbles are considered as storage medium and hot air from TFHE is used as hot fluid.

Assume the bed material has infinite thermal conductivity in the radial direction and zero conductivity in the axial flow direction. Also, assume no varying heat transfer coefficient with time and space inside the bed. However, Thermal conductivity can be semi-infinite in the direction of flow. A separate energy balance for bed material and water can be approximated for an element and time as expressed in Eqs. 7 and 8 [10].

$$(1 - \varepsilon)\rho_s c_{ps} \frac{\partial T_s}{\partial t} = h_v(T_f - T_s) \quad (7)$$

$$\varepsilon\rho_f c_{pf} \frac{\partial T_f}{\partial t} + \frac{4\dot{m}c_{pf}}{\pi D^2} \frac{\partial T_f}{\partial x} = h_v(T_s - T_f) \quad (8)$$

where ε is void fraction, h_v is the volumetric heat transfer coefficient, ρ_s , ρ_f are densities of the solid and fluid and c_{ps} , c_{pf} are respective specific heats. Diameter of the storage unit is denoted as D and \dot{m} is rate of airflow in the storage unit. T_s , T_f are temperature of storage material (alumina particles in this case) and fluid (air in this case), respectively.

Assuming the storage system is well insulated and neglecting heat losses, two dimensionless parameters time τ and dimensionless distance X can be written as

$$\tau = \frac{h_v t}{\rho_s c_{ps} (1 - \varepsilon)} \quad (9)$$

$$X = \frac{\pi D^2 h_v x}{4\dot{m}c_{pf}} \quad (10)$$

With simplification, Eqs. (7) and (8) can be written as

$$\frac{\partial T_s}{\partial \tau} = T_f - T_s \quad (11)$$

$$\frac{\partial T_s}{\partial X} = T_s - T_f \quad (12)$$

With assumption of initial temperature of solid medium at T_i , dimensionless temperature distribution may be obtained

$$\frac{T_s - T_i}{T_{fi} - T_i} = 1 - \exp^{-(X+\tau)} \sum_{n=0}^{n=\infty} X^n M_n(X\tau) \quad (13)$$

$$\frac{T_f - T_i}{T_{fi} - T_i} = 1 - \exp^{-(X+\tau)} \sum_{n=1}^{n=\infty} X^n M_n(X\tau) \quad (14)$$

where,

$$M_n(X\tau) = \sum_{k=0}^{k=\infty} \frac{(X\tau)^k}{k!(k+n)!} \quad (15)$$

T_{fi} is initial fluid temperature while entering the storage unit. Volumetric heat transfer coefficient, h_v can be calculated with the correlation given in Eq. 16 [11].

$$\frac{h_v d^2}{k_f} = 1.45(\text{Re}_d)^{0.7} \quad (16)$$

where Reynolds number is as follows

$$\text{Re}_d = Gd/\mu_f \quad (17)$$

where G is mass flux and d is equivalent spherical diameter. μ_f is the dynamic viscosity of the working fluid.

3 Results and Discussion

This section highlights key results of the simulation on the modelling equations mentioned in the previous section. The geometrical parameters and assumed operating parameters are mentioned in Table 1.

The solar and atmospheric data assumed for present analysis are based on weather data concerned to Indian climatic conditions. The absorber plate and tube data are considered based on the realistic conditions. Glass cover transmissivity and

absorptivity-related optical efficiency value can be taken as 0.85. Based on the thermal modelling mentioned in earlier sections, temperature of the outlet fluid and efficiency are obtained and presented.

The variation of instantaneous efficiency of flat plate solar collectors with respect to the heat energy absorbed by the absorber plate is illustrated in Fig. 2. Here, the efficiency value is 31% initially and increases to 71%. In the meantime, the solar radiation increased from 500 to 900 W/m². Moreover, the atmospheric temperature surrounding the collector increases at a lower pace. The outlet fluid temperature for different levels of heat energy absorbed in absorber plate vis-a-vis varying atmospheric temperature levels is as shown in Fig. 3. The trend seems to be almost linear kind for the both cases. The fluid temperature at the outlet increases with variations in solar radiance and atmospheric temperature.

The temperature distribution obtained analytically of three fluids along the length of the TFHE for parallel flow regime is presented in Fig. 4. The mass flow rates in three pipes are varied in such a way so as to attain air temperature 50 °C. The hot air from TFPE is being used to charge the storage medium.

Figure 5 depicts the temperature variation in the storage medium. The bed and the fluid temperature variation have been established. The graph represents the temperature along the storage section after 10 min. It is seen that temperature decreases along the length of the flow for both the storage medium and fluid. Packed bed types mainly alumina pebbles were used for storage of thermal energy. Hot air at 50 °C was used for fluid temperature during charging time where initial temperature was maintained at 20 °C. Future work may be oriented on experimentation of such solar

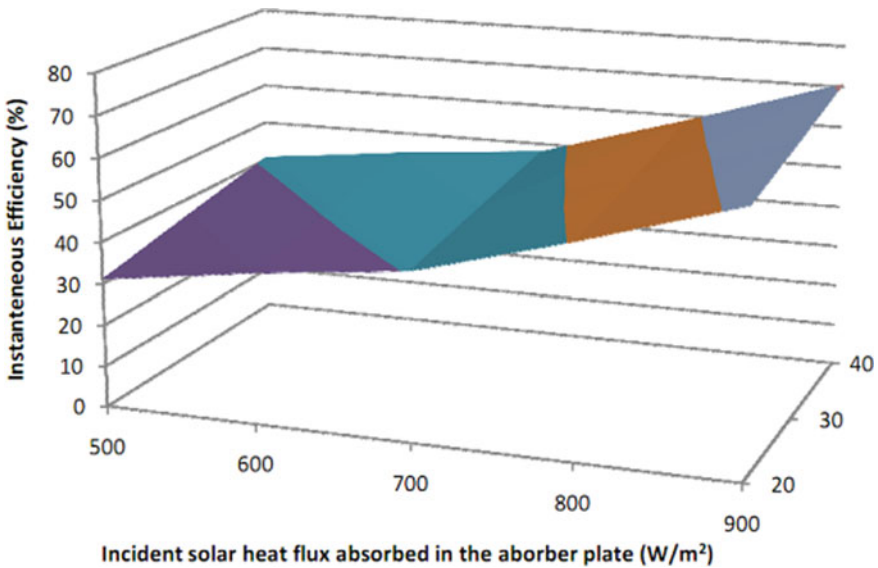


Fig. 2 Efficiency variation vs. Incident solar heat flux versus atmospheric temperature

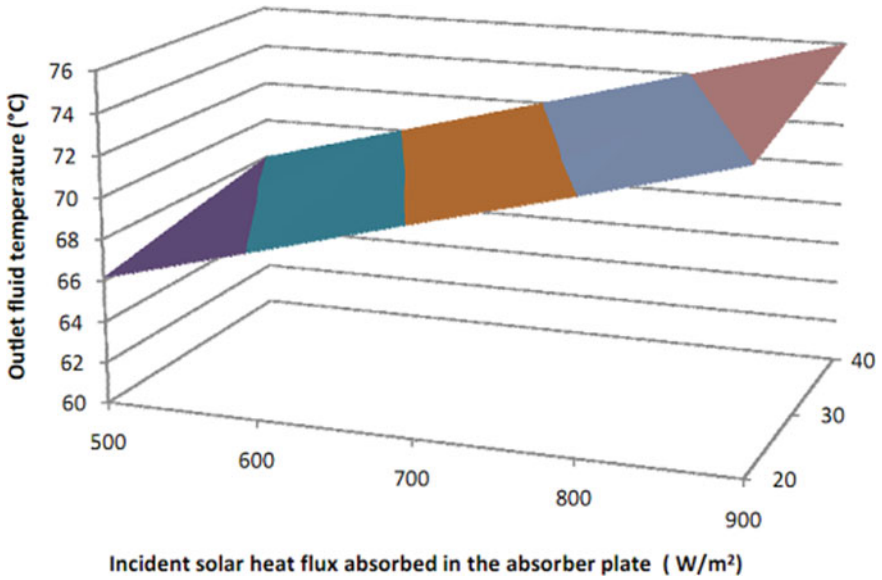


Fig. 3 Outlet fluid temperature variation versus incident solar heat flux versus atmospheric temperature

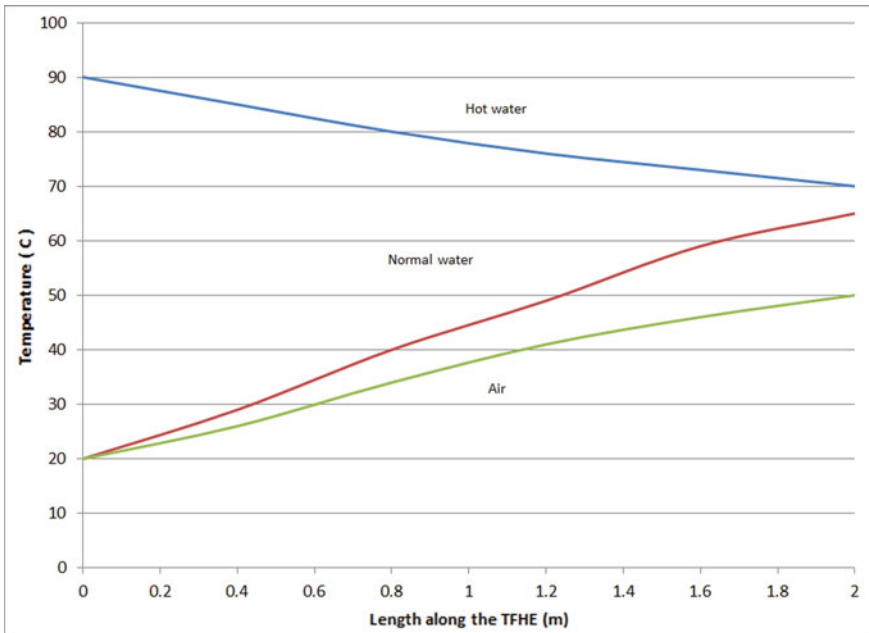


Fig. 4 Variation of temperature in multi-fluid heat exchanger

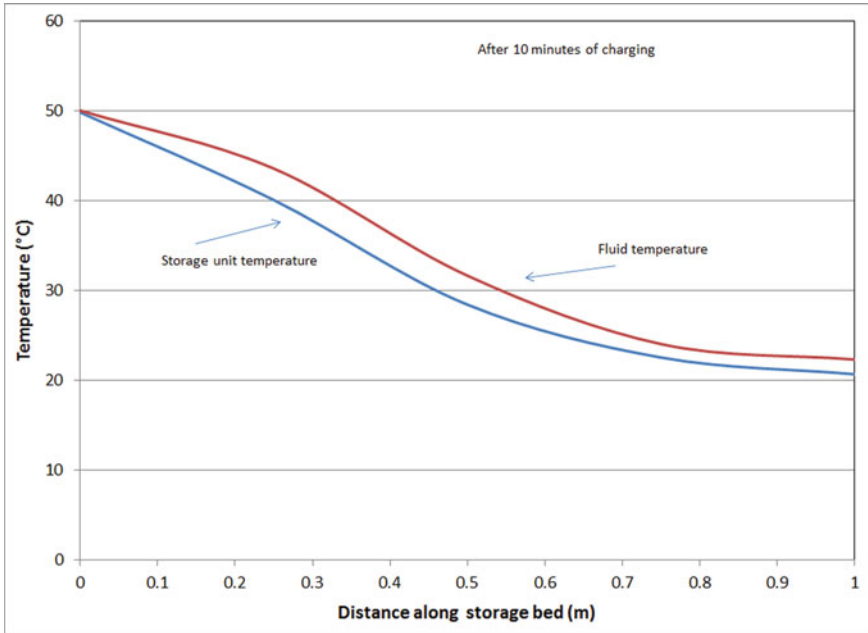


Fig. 5 Fluid temperature variation in the storage medium

thermal systems for simultaneous heating of water and air as well as storage for night time applications.

4 Conclusions

In search of efficient solar energy harvesting, combined effect can make the system most efficient. Analysis by heat transfer modelling of flat plate collector coupled with multi-fluid heat exchanger and heat storage system is interesting. Outlet fluid temperature for different solar energy absorbed by the plate along with the ambient temperature values were recorded accurately. FPSC was integrated with TFHE for attaining hot air and hot water. Hot air from TFPE was used for energy storage in STSS. Major observation in this work is that instantaneous efficiency can rise up to 71% at solar radiation of 900 W/m². Increased efficiency value can be attributed to atmospheric temperature rising at a slower pace.

References

1. Kalogirou SA (2004) Solar thermal collectors and applications. *Prog Energy Combust Sci* 30:231–295
2. Alghoul MA, Sulaiman MY, Azmi BZ, Wahab MAbd (2005) Review of materials for solar thermal collectors. *Anti-Corros Methods Mater* 52:199–206
3. Ayompe LM, Duffy A (2013) Analysis of the thermal performance of solar water heating system with flat plate collectors in a temperate climate. *Appl Therm Eng* 58:447–454
4. Farahat S, Sarhaddi F, Ajam H (2009) Exergetic optimization of flat plate solar collectors. *Renew Energy* 34:1169–1174
5. Karim MA, Hawalder MNA (2004) Development of solar air collectors for drying applications. *Energy Convers Manage* 45:329–344
6. Edwards J, Bindra H (2017) An experimental study on storing thermal energy in packed beds with saturated steam as heat transfer fluid. *Sol Energy* 157:456–461
7. Kalaiarasi G, Velraj R, Swami MV (2016) Experimental energy and exergy analysis of a flat plate solar air heater with a new design of integrated sensible heat storage. *Energy* 111:609–619
8. *Solar Radiation Handbook* (2008) MNRE and IMD, India
9. Mohanty S, Rout A, Patra PK, Sahoo SS (2017) Soft computing techniques for a solar collector using solar radiation data. *Energy Proc* 109
10. Sukhatme SP, Nayak JK (2008) *Principle of thermal collection and storage*, 3rd Edn. Tata McGraw-Hill Publishing Company Limited
11. Mohapatra T, Padhi BN, Sahoo SS (2017) Experimental investigation of convective heat transfer in an inserted coiled tube type three fluid heat exchanger. *Appl Therm Eng* 117:297–307